

should exist for chlorine and phosphorus in the monocarbonyl compound. The presence of only one isomer is confirmed by the NMR spectra. Due to coordination to the metal the $\nu(\text{NH})$ frequency has decreased to 3160 cm^{-1} .

In spite of the easy migration of the N-H proton in **1**, we did not observe the evolution of hydrogen chloride in the reactions of $\text{C}_5\text{H}_5\text{Mo}(\text{CO})_3\text{Cl}$, even in the presence of pyridine.

In summary, the reaction of $(\eta^5\text{-C}_5\text{H}_5)\text{Mo}(\text{CO})_3\text{H}$ in THF with the bicyclic phosphorane **1** (abbreviated phoran) gives $\text{C}_5\text{H}_5\text{Mo}(\text{CO})_2(\text{phoran})\text{H}$, **2**, which slowly converts in CHCl_3 solution to $\text{C}_5\text{H}_5\text{Mo}(\text{CO})_2(\text{phoran})\text{Cl}$, **3**. The same product can also be obtained from $\eta^5\text{-C}_5\text{H}_5\text{Mo}(\text{CO})_3\text{Cl}$ and **1** in diethyl ether. Although a cationic form $[\text{C}_5\text{H}_5\text{Mo}(\text{CO})_2(\text{phoran})]\text{Cl}$ of **3** may exist in traces, **3** can be converted in good yields into the $[\text{C}_5\text{H}_5\text{Mo}(\text{CO})_2(\text{phoran})]\text{PF}_6$ salt (**5**) by addition of NH_4PF_6 in aqueous ethanol. Reflux of **3** in benzene results in a further substitution of CO to give $\text{C}_5\text{H}_5\text{Mo}(\text{CO})(\text{phoran})\text{Cl}$, **4**. The ligand is monodentate and phosphorus-bound in **2** and **3** and bidentate in **4** and **5**, as shown in the ^1H , ^{13}C , and ^{31}P NMR.

Acknowledgment. We thank Dr. Bernard Septe for measuring the NMR spectra.

Contribution from the Department of Chemistry,
University of Minnesota, Minneapolis, Minnesota 55455

Chemical and X-ray Structural Properties of Bis[bis(diphenylphosphino)methane]carbonylrhodium(I) Tetrafluoroborate

L. H. Pignolet,*¹ D. H. Doughty, S. C. Nowicki,
and A. L. Casalnuovo²

Received January 10, 1980

Recent studies on the catalytic properties of metal complexes with chelating diphosphine ligands have shown rather large rate and selectivity effects as a function of the diphosphine chelate ring size.³⁻⁵ Specific studies have involved hydroformylation using a platinum-diphosphine-tin system,³ hydrogenation using a rhodium chloride-diphosphine system,⁴ and decarbonylation of aldehydes using a cationic bis(diphosphine)rhodium system.^{5,6} In these cases where diphosphines of the type $\text{Ph}_2\text{P}(\text{CH}_2)_n\text{PPh}_2$ with $n = 1-6$ were used, the catalytic rates showed maxima for values of n ranging from 3 to 5. Clearly a combination of chelate ring strain, flexibility, and electronic bonding properties is important.

During our studies on the catalytic decarbonylation of aldehydes using $\text{Rh}[\text{Ph}_2(\text{CH}_2)_n\text{PPh}_2]_2^+$ complexes with $n = 1-6$, it became apparent that the value of n played a major role in determining reactivity and selectivity.^{5,6} In this reaction the lability of CO from the intermediate $\text{Rh}[\text{Ph}_2\text{P}(\text{CH}_2)_n\text{PPh}_2]_2\text{CO}^+$ is important and in some cases may be the rate-determining step.⁷ Therefore, we set out to characterize these carbonyl complexes for $n = 1$ (dppm), 3 (dppp), and 4 (dppb). The $n = 2$ (dppe) analogue cannot be prepared⁸

whereas the dppm and dppp complexes are readily formed at $25\text{ }^\circ\text{C}$ in solution by reaction of CO gas with bis(diphosphine)rhodium tetrafluoroborate. This reaction is reversible. The reaction of CO with $\text{Rh}(\text{dppb})_2^+$ leads to dimeric products $\text{Rh}_2(\text{dppb})_3(\text{CO})_x$ with $x = 2, 3$, and 4. The characterization and structural properties of the dppb complexes will be published elsewhere.⁹ The chemical and ^{31}P NMR properties of $\text{Rh}(\text{dppm})_2\text{CO}^+$ and $\text{Rh}(\text{dppp})_2\text{CO}^+$ and the single-crystal X-ray structure of the former are presented here. The solid-state structure of $[\text{Rh}(\text{dppm})_2\text{CO}]\text{BF}_4$ is only the second crystallographic example of dppm chelating to a single Rh atom.¹⁰

Experimental Section

$^{31}\text{P}\{^1\text{H}\}$ NMR spectra were recorded at 40.5 MHz by using a Varian Associates XL-100 FT instrument, and chemical shifts are referenced to external standard 85% H_3PO_4 with positive shifts in parts per million upfield. Infrared spectra were recorded on a Perkin-Elmer Model 283 spectrometer. Hydrated rhodium(III) chloride was obtained on loan from Matthey Bishop, Inc., and bis(diphenylphosphino)methane (dppm) and 1,3-bis(diphenylphosphino)propane (dppp) were purchased from Strem Chemicals.

Synthesis of Compounds. $[\text{Rh}(\text{dppm})_2]\text{BF}_4$. $\text{Rh}_2\text{Cl}_2(\text{COD})_2$ (COD = 1,5-cyclooctadiene)¹¹ (140 mg, 0.57 mmol) was stirred in 25 mL of acetone under a purified N_2 atmosphere. Upon addition of AgBF_4 (128 mg, 0.66 mmol) to this slurry, the rhodium complex dissolved, and a white precipitate formed, leaving a pale yellow solution. This solution was refluxed for 30 min and filtered. The filtrate was added to a toluene solution (30 mL) of dppm (438 mg, 1.14 mmol), giving an orange color. Slow evaporation of the acetone yielded orange-red crystals. All the above manipulations were carried out under a N_2 atmosphere by using standard Schlenk techniques. The compound is air sensitive and may be recrystallized from dichloromethane-diethyl ether. Anal. Calcd for $\text{RhC}_{50}\text{H}_{44}\text{P}_4\text{BF}_4$: C, 62.65; H, 4.59. Found: C, 62.95; H, 4.55. $^{31}\text{P}\{^1\text{H}\}$ NMR (25 $^\circ\text{C}$, acetone- d_6): δ 23.2, (d, $J_{\text{Rh-P}} = 116$ Hz).

$[\text{Rh}(\text{dppm})_2\text{CO}]\text{BF}_4$. Gaseous CO was bubbled through a dichloromethane solution of $[\text{Rh}(\text{dppm})_2]\text{BF}_4$ for ca. 15 min. The color changed from orange to yellow after ca. 5 min. Gold crystals were obtained upon the addition of diethyl ether under a CO atmosphere. IR (KBr disk): $\nu(\text{CO})$ 1945 cm^{-1} . Anal. Calcd for $\text{RhC}_5\text{H}_{44}\text{OP}_4\text{BF}_4$: C, 62.09; H, 4.46. Found: C, 61.79; H, 4.67. $^{31}\text{P}\{^1\text{H}\}$ NMR (25 $^\circ\text{C}$, acetone- d_6): δ 22.5 (d, $J_{\text{Rh-P}} = 98$ Hz).

$[\text{Rh}(\text{dppp})_2\text{CO}]\text{BF}_4$ was prepared in a manner analogous to that for the dppm complex from $[\text{Rh}(\text{dppp})_2]\text{BF}_4$.⁵ IR (KBr disk): $\nu(\text{CO})$ 1929 cm^{-1} . Anal. Calcd for $\text{RhC}_{55}\text{H}_{52}\text{OP}_4\text{BF}_4$: C, 63.35; H, 4.99. Found: C, 62.98; H, 5.44. $^{31}\text{P}\{^1\text{H}\}$ NMR ($-80\text{ }^\circ\text{C}$, acetone- d_6): δ -14.27 and 13.28 (A_2B_2X pattern, $J_{\text{Rh-P}} = 86$ and 113 Hz, $J_{\text{P-P}} = 45$ Hz, in good agreement with the literature values).⁸

X-ray Structure Determination. A crystal of $[\text{Rh}(\text{dppm})_2\text{CO}]\text{BF}_4$ was fastened to the end of a thin glass fiber with 5-min epoxy resin. The dimensions of this ca. rectangular crystal were $0.25 \times 0.20 \times 0.20$ mm. The crystal class was found to be monoclinic by the automatic peak searching, centering, and indexing routines of the Enraf-Nonius SDP-CAD 4 system.¹² A Delaunay reduction calculation (program TRACER)¹² did not indicate a higher symmetry, and the monoclinic crystal class was verified by examination of the intensities of numerous reflections required to be equivalent by the $2/m$ crystal symmetry. The space group $P2_1/c$ was chosen due to the systematic absences in the data ($h0l$, $l = 2n + 1$, and $0k0$, $k = 2n + 1$) and was used to successfully solve and refine the structure (vide infra). The unit cell dimensions were determined by least-squares refinement of the angular values of 25 Mo $K\alpha$ ($\lambda = 0.71069\text{ \AA}$) peaks centered on a CAD 4 diffractometer¹² and are $a = 11.281(2)\text{ \AA}$, b

(1) To whom correspondence should be addressed.

(2) Lando Summer Research Fellow, 1979.

(3) Kawabata, Y.; Hayashi, T.; Ogata, I. *J. Chem. Soc., Chem. Commun.* **1979**, 462.

(4) Poulin, J.-C.; Dang, T.-P.; Kagan, H. B. *J. Organomet. Chem.* **1975**, *84*, 87.

(5) Doughty, D. H.; Pignolet, L. H. *J. Am. Chem. Soc.* **1978**, *100*, 7083.

(6) Doughty, D. H.; McGuiggan, M. F.; Wang, H.; Pignolet, L. H. In "Fundamental Research in Homogeneous Catalysis"; Plenum: New York, 1979; Vol. 3, p 909.

(7) Doughty, D. H. Ph.D. Thesis, University of Minnesota, 1979.

(8) Sanger, A. R. *J. Chem. Soc., Dalton Trans.* **1977**, 120.

(9) Doughty, D. H.; Nowicki, S. C.; Pignolet, L. H., to be submitted for publication.

(10) Cowie, M.; Dwight, S. K. *Inorg. Chem.* **1979**, *18*, 1209.

(11) Chatt, J.; Venanzi, L. M. *J. Chem. Soc. A* **1957**, 4735.

(12) All calculations were carried out on PDP 8A and 11/34 computers using the Enraf-Nonius CAD 4-SDP programs. This crystallographic computing package is described in the following references: Frenz, B. A. In "Computing in Crystallography"; Schenk, H., Olthof-Hazekamp, R., van Koningsveld, H., Bassi, G. C., Eds.; Delft University Press: Delft, Holland, 1978; pp 64-71; "CAD 4 SDP Users Manual"; Enraf-Nonius: Delft, Holland, 1978.

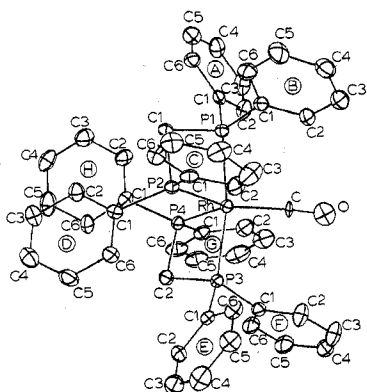


Figure 1. ORTEP drawing of the cation $\text{Rh}(\text{dppm})_2\text{CO}^+$ showing the labeling scheme.

$a = 19.039$ (4) Å, $c = 22.083$ (4) Å, $\beta = 101.78$ (2)°, and $V = 4643$ Å³. The measured density of 1.40 g/cm³ (floatation) agrees with the calculated density of 1.425 g/cm³ with $Z = 4$ and molecular formula $\text{RhC}_{51}\text{H}_{44}\text{OP}_4\text{BF}_4$ ($M_r = 996.5$). A total of 8255 unique reflections were measured in the scan range $2\theta = 0-50^\circ$ on a CAD 4 automatic diffractometer using graphite-monochromatized Mo $K\alpha$ radiation and employing a variable rate $\omega-2\theta$ scan technique. Background counts were measured at both ends of the scan range by using a scan equal, at each side, to one-fourth of the scan range of the peak. In this manner, the total duration of measuring backgrounds is equal to half of the time required for the peak scan. The intensities of three standard reflections were measured every 1.5 h of X-ray exposure, and no decay with time was noted. After correction for Lorentz, polarization, and background effects but not for absorption ($\mu = 5.5$ cm⁻¹) effects,¹³ 4906 reflections were judged observed [$F_o^2 \geq 2.5\sigma(F_o^2)$] and were used in all subsequent calculations.¹³ Conventional heavy-atom techniques were used to solve the structure, and refinement with all nonhydrogen atoms thermally anisotropic by full-matrix least-squares methods (560 variables) converged R and R_w to their final values of 0.053 and 0.074, respectively.¹⁴ The atomic scattering factors were taken from the usual tabulation,¹⁵ and the effects of anomalous dispersion were included in F_o for Rh and P by using Cromer and Ibers¹⁶ values of $\Delta f'$ and $\Delta f''$. The error in an observation of unit weight was 1.35 with a value of 0.05 for p in the $\sigma(I)$ equation.¹³ The final difference Fourier map did not reveal any chemically significant features other than some hydrogen positions which were not included in any calculations.

The final atomic coordinates with their estimated standard deviations and the final thermal parameters are given in Tables I and II (Table II given as supplementary material). An ORTEP perspective of the cation which includes the labeling scheme is presented in Figure 1. A table of observed and calculated structure factor amplitudes is available.¹⁷

Results and Discussion

The five-coordinate complexes $[\text{Rh}(\text{dppm})_2\text{CO}]\text{BF}_4$ and $[\text{Rh}(\text{dppp})_2\text{CO}]\text{BF}_4$ have been synthesized by reaction of CO

gas at 1 atm with the four-coordinate cationic bis(diphenylphosphine)rhodium(I) complexes in CH_2Cl_2 solution at 25 °C (eq 1; L-L = dppm or dppp). Reaction 1 is reversible, and



purging of the solution with N_2 at elevated temperatures readily removes the coordinated CO. This reaction is conveniently monitored by IR spectroscopy, and the relative lability of CO from these five-coordinate complexes has been determined. CH_2Cl_2 solutions of $\text{Rh}(\text{L-L})_2\text{CO}^+$ were vigorously purged with N_2 at 25 °C for ca. 30 min, and IR analysis revealed that the dppp complex lost nearly all (>90%) of the coordinated CO while the dppm complex lost very little (<10%). Therefore, CO is much more labile from $\text{Rh}(\text{dppp})_2\text{CO}^+$ in CH_2Cl_2 solution than from $\text{Rh}(\text{dppm})_2\text{CO}^+$, even though a comparison of $\nu(\text{CO})$ stretching frequencies (1929 and 1945 cm⁻¹, respectively) indicates that the Rh-CO bond is stronger in the dppp compound. Obviously, the lability of CO is dependent on factors other than the Rh-CO bond strength in $\text{Rh}(\text{L-L})_2\text{CO}^+$ and must be due to energy differences between ground and transition states caused by chelate ring strain effects. Indeed, $\text{Rh}(\text{dppe})_2^+$ is unreactive toward CO in CH_2Cl_2 solution at 25 °C and CO pressure up to 100 psig. This lack of reactivity is probably due to the greater stability of $\text{Rh}(\text{L-L})_2^+$ with the strain-free five-membered chelate ring of dppe compared to the more strained four- and six-membered dppm and dppp chelate rings. Similar observations are known in Ir chemistry where $\text{Ir}(\text{dppm})_2^+$ forms a dioxygen adduct much more readily than does $\text{Ir}(\text{dppe})_2^+$.¹⁸

The geometry of $\text{Rh}(\text{L-L})_2\text{CO}^+$ complexes is assumed to be close to trigonal bipyramidal (TBP) with the CO ligand in an equatorial position. This conclusion derives from X-ray (L-L = dppe)¹⁹ and ³¹P NMR (L-L = dppe, dppp)²⁰ data on analogous Ir complexes which are consistent with this stereochemistry. The ³¹P{¹H} NMR spectra of $\text{Rh}(\text{dppp})_2\text{CO}^+\text{BF}_4^-$ in acetone-*d*₆ solution saturated with CO shows two broad resonances at ambient temperature ($\delta -15$ and 10 vs. external 85% H_3PO_4 with positive shifts upfield) which sharpen into an $\text{A}_2\text{B}_2\text{X}$ pattern at -70 °C (see Experimental Section). The $\text{A}_2\text{B}_2\text{X}$ pattern is consistent with a TBP geometry with CO equatorial, and the broadening at high temperature suggests fluxionality. The ³¹P{¹H} NMR spectra of $\text{Rh}(\text{dppm})_2\text{CO}^+$ in acetone-*d*₆ solution saturated with CO shows a sharp doublet down to -80 °C ($\delta 22.5$, $J_{\text{Rh-P}} = 98$ Hz), indicating rapid intramolecular rearrangement of a TBP structure or possibly a square-pyramidal (SP) structure with CO axial. Similar observations have been made with $\text{Ir}(\text{dppm})_2\text{CO}^+$, $\text{Ir}(\text{dppe})_2\text{CO}^+$, and $\text{Ir}(\text{dppp})_2\text{CO}^+$ where the barrier to intramolecular rearrangement, presumably via a TBP-SP-TBP mechanism, decreases in the order dppp > dppe > dppm.²⁰ It is clear that the effect of chelate ring size is important in determining the dynamics of the rearrangement. Kepert²¹ has concluded that decreasing the "bite" parameter b [$\text{P}\cdots\text{P}$ distance/ M-P distance] decreases the energy separation between the more stable TBP and the less stable SP geometry, and as b becomes very small, the SP geometry may actually become favored.

In order to directly measure the stereochemical effects of ring strain in a five-coordinate dppm complex of Rh(I), we determined the single-crystal X-ray structure of $[\text{Rh}(\text{dppm})_2\text{CO}]\text{BF}_4$. Also, since only one X-ray structure containing a dppm ligand chelated to a single Rh atom has been

(13) The intensity data were processed as described in: "CAD4 and SDP Users Manual"; Enraf-Nonius, Delft, Holland, 1978. The net intensity I is given as $I = (K/\text{NPI})(C - 2B)$, where $K = 20.1166 \times$ (attenuator factor), $\text{NPI} =$ ratio of fastest possible scan rate to scan rate for the measurement, $C =$ total count, and $B =$ total background count. The standard deviation in the net intensity is given by $\sigma^2(I) = (K/\text{NPI})^2[C + 4B + (pI)^2]$, where p is a factor used to downweight intense reflections. The observed structure factor amplitude F_o is given by $F_o = (I/Lp)^{1/2}$, where $Lp =$ Lorentz and polarization factors. The $\sigma(I)$'s were converted to the estimated errors in the relative structure factors $\sigma(F_o)$ by $\sigma(F_o) = 1/2(\sigma(I)/I)F_o$.

(14) The function minimized was $\sum w(|F_o| - |F_c|)^2$ where $w = 1/\sigma^2(F_o)$. The unweighted and weighted residuals are defined as follows: $R = (\sum ||F_o| - |F_c||) / (\sum |F_o|)$ and $R_w = [(\sum w(|F_o| - |F_c|)^2) / (\sum w|F_o|)^2]^{1/2}$. The error in an observation of unit weight is $[\sum w(|F_o| - |F_c|)^2 / (\text{NO} - \text{NV})]^{1/2}$, where NO and NV are the number of observations and variables, respectively.

(15) Cromer, D. T.; Waber, J. T. "International Tables for X-ray Crystallography"; Kynoch Press: Birmingham, England, 1974; Vol. IV, Table 2.2.A.

(16) Table 2.3.1 in ref 15.

(17) See paragraph at end of paper regarding supplementary material.

(18) Nolte, M.; Singleton, E.; Laing, M. *J. Chem. Soc., Dalton Trans.* **1976**, 1979.

(19) Jarvis, J. A. J.; Mais, R. H. B.; Owston, P. G.; Taylor, K. A. *Chem. Commun.* **1966**, 906.

(20) Miller, J. S.; Caulton, K. G. *J. Am. Chem. Soc.* **1975**, *97*, 1067.

(21) Kepert, D. L. *Inorg. Chem.* **1973**, *12*, 1942.

Table I. Positional and Thermal Parameters and Their Estimated Standard Deviations^a

atom	x	y	z	B ₁₁	B ₂₂	B ₃₃	B ₁₂	B ₁₃	B ₂₃
Rh	-0.06949 (4)	0.20708 (3)	0.05190 (2)	0.00621 (3)	0.00254 (1)	0.00142 (1)	-0.00052 (5)	0.00147 (3)	-0.00037 (2)
P1	-0.2672 (1)	0.20009 (9)	0.06655 (7)	0.0067 (1)	0.00243 (5)	0.00243 (5)	-0.0011 (1)	0.0020 (1)	-0.0017 (7)
P2	-0.1512 (1)	0.32096 (9)	0.05375 (7)	0.0065 (1)	0.00232 (5)	0.00167 (3)	-0.0001 (1)	0.0017 (1)	0.00039 (7)
P3	0.1282 (1)	0.23338 (10)	0.04759 (7)	0.0063 (1)	0.00268 (5)	0.00156 (3)	-0.0004 (1)	0.0017 (1)	-0.00040 (7)
P4	0.0514 (2)	0.20613 (10)	0.15391 (7)	0.0070 (1)	0.00278 (5)	0.00160 (3)	-0.0002 (2)	0.0015 (1)	-0.00039 (8)
F1	-0.5389 (7)	0.3201 (4)	0.1539 (4)	0.0198 (8)	0.0097 (3)	0.0107 (3)	0.0078 (9)	-0.0112 (9)	-0.0083 (5)
F2	-0.3909 (8)	0.3467 (5)	0.2239 (4)	0.0292 (11)	0.0094 (4)	0.0084 (3)	-0.0045 (11)	-0.0128 (9)	-0.0022 (6)
F3	-0.5561 (11)	0.3998 (7)	0.2220 (5)	0.0740 (17)	0.0199 (6)	0.0107 (3)	0.0428 (13)	0.0272 (10)	-0.0038 (7)
F4	-0.4823 (15)	0.4127 (8)	0.1486 (8)	0.0494 (24)	0.0161 (7)	0.0182 (7)	0.0069 (22)	-0.0096 (23)	0.0137 (11)
O	-0.0707 (8)	0.0809 (5)	-0.0286 (4)	0.0195 (9)	0.0076 (4)	0.0060 (3)	-0.004 (1)	0.0044 (8)	-0.0034 (5)
C	-0.0747 (6)	0.1258 (4)	0.0020 (3)	0.0092 (6)	0.0031 (2)	0.0029 (1)	-0.0023 (6)	0.0032 (5)	-0.0050 (3)
C1	-0.2715 (6)	0.2909 (4)	0.0937 (3)	0.0079 (5)	0.0024 (2)	0.0021 (1)	-0.0019 (6)	0.0035 (4)	-0.0001 (3)
C2	0.1740 (6)	0.2570 (4)	0.1298 (3)	0.0090 (6)	0.0037 (2)	0.0014 (1)	-0.0021 (7)	0.0016 (5)	-0.0003 (3)
C1A	-0.3099 (6)	0.1442 (3)	0.1246 (3)	0.0079 (5)	0.0024 (2)	0.0015 (1)	-0.0026 (5)	0.0009 (4)	-0.0003 (3)
C2A	-0.2558 (8)	0.0776 (4)	0.1353 (3)	0.0155 (5)	0.0027 (2)	0.0024 (2)	0.0011 (8)	0.0038 (6)	0.0003 (3)
C3A	-0.2919 (10)	0.0338 (4)	0.1788 (4)	0.0224 (12)	0.0029 (2)	0.0029 (2)	-0.0006 (10)	0.0051 (8)	0.0005 (4)
C4A	-0.3773 (8)	0.0549 (5)	0.2123 (4)	0.0176 (10)	0.0036 (3)	0.0024 (2)	-0.0029 (9)	0.0037 (7)	-0.0001 (4)
C5A	-0.4275 (8)	0.1214 (5)	0.2028 (3)	0.0128 (8)	0.0047 (3)	0.0022 (2)	-0.0033 (8)	0.0031 (6)	0.0008 (4)
C6A	-0.3950 (7)	0.1670 (4)	0.1584 (3)	0.0087 (6)	0.0040 (3)	0.0022 (2)	-0.0017 (7)	0.0028 (5)	-0.0003 (4)
C1B	-0.3838 (6)	0.1920 (4)	-0.0029 (3)	0.0068 (5)	0.0034 (2)	0.0020 (1)	-0.0012 (6)	0.0020 (4)	-0.0004 (3)
C2B	-0.3678 (7)	0.1425 (5)	-0.0475 (4)	0.0095 (7)	0.0043 (3)	0.0027 (2)	-0.0008 (8)	0.0002 (6)	-0.0022 (4)
C3B	-0.4488 (8)	0.1383 (6)	-0.1043 (4)	0.0105 (8)	0.0066 (4)	0.0032 (2)	-0.0007 (10)	0.0001 (7)	-0.0027 (5)
C4B	-0.5468 (9)	0.1850 (6)	-0.1162 (4)	0.0111 (8)	0.0065 (4)	0.0033 (2)	-0.0032 (10)	0.0012 (8)	-0.0010 (5)
C5B	-0.5661 (8)	0.2316 (6)	-0.0710 (4)	0.0111 (8)	0.0056 (4)	0.0035 (2)	0.0015 (10)	-0.0027 (8)	-0.0008 (5)
C6B	-0.4841 (7)	0.2341 (5)	-0.0139 (4)	0.0078 (7)	0.0048 (3)	0.0031 (2)	0.0022 (8)	0.0004 (6)	-0.0002 (4)
C1C	-0.2381 (6)	0.3579 (4)	-0.0171 (3)	0.0066 (5)	0.0030 (2)	0.0021 (1)	0.0003 (6)	0.0021 (4)	0.0014 (3)
C2C	-0.2441 (7)	0.3228 (5)	-0.0730 (3)	0.0105 (7)	0.0052 (3)	0.0016 (1)	0.0020 (8)	0.0010 (5)	-0.0001 (4)
C3C	-0.3190 (8)	0.3517 (6)	-0.1266 (4)	0.0140 (9)	0.0076 (4)	0.0022 (2)	0.0086 (10)	0.0001 (7)	0.0005 (5)
C4C	-0.3874 (8)	0.4103 (5)	-0.1240 (4)	0.0109 (8)	0.0065 (4)	0.0023 (2)	0.0045 (9)	0.0006 (6)	0.0019 (4)
C5C	-0.3819 (8)	0.4441 (5)	-0.0685 (4)	0.0113 (8)	0.0040 (3)	0.0030 (2)	0.0029 (8)	0.0008 (7)	0.0020 (4)
C6C	-0.3068 (7)	0.4192 (4)	-0.0146 (4)	0.0107 (7)	0.0034 (2)	0.0026 (2)	0.0022 (7)	0.0012 (6)	0.0007 (4)
C1D	-0.0748 (6)	0.3953 (3)	0.0953 (3)	0.0064 (5)	0.0024 (2)	0.0021 (1)	-0.0002 (5)	0.0010 (5)	0.0008 (3)
C2D	-0.0920 (7)	0.4164 (4)	0.1529 (3)	0.0122 (8)	0.0032 (2)	0.0020 (2)	-0.0005 (7)	0.0017 (6)	-0.0003 (3)
C3D	-0.0193 (8)	0.4702 (4)	0.1860 (4)	0.0138 (9)	0.0031 (2)	0.0027 (2)	-0.0020 (8)	0.0006 (7)	-0.0003 (4)
C4D	0.0663 (8)	0.5027 (5)	0.1608 (4)	0.0124 (9)	0.0033 (3)	0.0039 (3)	-0.0014 (8)	0.0007 (8)	-0.0002 (5)
C5D	0.0808 (7)	0.4835 (4)	0.0999 (4)	0.0105 (7)	0.0033 (3)	0.0042 (2)	-0.0033 (7)	0.0038 (7)	0.0001 (4)
C6D	0.0107 (7)	0.4305 (4)	0.0682 (4)	0.0096 (7)	0.0030 (2)	0.0034 (2)	-0.0014 (7)	0.0036 (6)	-0.0007 (4)
C1E	0.1693 (6)	0.3041 (3)	0.0003 (3)	0.0067 (5)	0.0025 (2)	0.0020 (1)	0.0013 (5)	0.0026 (4)	-0.0003 (3)
C2E	0.2715 (7)	0.3431 (4)	0.0210 (3)	0.0111 (7)	0.0026 (2)	0.0028 (2)	-0.0026 (6)	0.0037 (5)	-0.0008 (3)
C3E	0.3037 (9)	0.3935 (5)	-0.0186 (4)	0.0173 (9)	0.0035 (3)	0.0038 (2)	-0.0023 (9)	0.0074 (7)	0.0001 (4)
C4E	0.2328 (10)	0.4027 (4)	-0.0791 (4)	0.0244 (12)	0.0030 (3)	0.0040 (2)	0.0022 (10)	0.0086 (8)	0.0021 (4)
C5E	0.1339 (8)	0.3627 (5)	-0.0979 (4)	0.0144 (9)	0.0036 (3)	0.0030 (2)	0.0017 (9)	0.0030 (7)	0.0019 (4)
C6E	0.0984 (7)	0.3130 (4)	-0.0590 (3)	0.0117 (7)	0.0034 (2)	0.0022 (2)	0.0026 (7)	0.0032 (5)	0.0008 (3)
C1F	0.2202 (6)	0.1600 (4)	0.0316 (3)	0.0070 (5)	0.0025 (2)	0.0023 (1)	0.0002 (6)	0.0021 (5)	-0.0001 (3)
C2F	0.1969 (8)	0.1344 (4)	-0.0284 (4)	0.0168 (9)	0.0038 (3)	0.0025 (2)	0.0059 (8)	0.0013 (7)	-0.0008 (4)
C3F	0.2575 (10)	0.0781 (5)	-0.0449 (4)	0.0212 (11)	0.0041 (3)	0.0035 (2)	0.0063 (9)	0.0040 (8)	-0.0022 (4)
C4F	0.3461 (8)	0.0448 (5)	-0.0008 (4)	0.0105 (8)	0.0039 (3)	0.0038 (2)	0.0019 (8)	0.0031 (7)	-0.0011 (4)
C5F	0.3732 (8)	0.0722 (5)	0.0581 (4)	0.0095 (7)	0.0052 (3)	0.0040 (2)	0.0050 (8)	0.0019 (7)	-0.0009 (5)
C6F	0.3105 (7)	0.1304 (5)	0.0748 (4)	0.0080 (6)	0.0045 (3)	0.0030 (2)	0.0034 (7)	0.0010 (6)	-0.0009 (4)
C1G	0.1251 (6)	0.1231 (4)	0.1830 (3)	0.0092 (6)	0.0029 (2)	0.0023 (1)	0.0009 (6)	0.0039 (4)	0.0012 (3)
C2G	0.1007 (8)	0.0638 (4)	0.1474 (4)	0.0149 (9)	0.0028 (2)	0.0039 (2)	0.0003 (8)	0.0061 (7)	0.0007 (4)
C3G	0.1654 (10)	0.0006 (5)	0.1640 (5)	0.0171 (11)	0.0041 (3)	0.0054 (3)	0.0026 (10)	0.0074 (9)	0.0019 (5)
C4G	0.2529 (9)	0.0003 (6)	0.2197 (5)	0.0172 (10)	0.0057 (4)	0.0060 (3)	0.0061 (11)	0.0105 (8)	0.0033 (6)
C5G	0.2778 (8)	0.0592 (5)	0.2559 (5)	0.0115 (8)	0.0059 (4)	0.0042 (2)	0.0045 (9)	0.0047 (7)	0.0032 (5)
C6G	0.2134 (7)	0.1235 (5)	0.2375 (4)	0.0087 (7)	0.0052 (3)	0.0036 (2)	0.0027 (8)	0.0029 (6)	0.0029 (4)
C1H	0.0222 (6)	0.2492 (4)	0.2235 (3)	0.0084 (6)	0.0030 (2)	0.0015 (1)	0.0016 (6)	0.0009 (5)	0.0003 (3)
C2H	-0.0804 (7)	0.2324 (5)	0.2425 (3)	0.0110 (7)	0.0048 (3)	0.0017 (1)	0.0005 (8)	0.0027 (5)	0.0004 (3)
C3H	-0.1118 (8)	0.2671 (6)	0.2929 (4)	0.0127 (9)	0.0063 (4)	0.0022 (2)	0.0009 (10)	0.0027 (6)	-0.0003 (4)
C4H	-0.0373 (9)	0.3178 (5)	0.3232 (4)	0.0183 (10)	0.0045 (3)	0.0021 (2)	0.0067 (9)	0.0042 (7)	0.0008 (4)
C5H	0.0605 (10)	0.3358 (5)	0.3037 (4)	0.0248 (13)	0.0038 (3)	0.0023 (2)	-0.0001 (11)	0.0028 (8)	-0.0003 (4)
C6H	0.0996 (8)	0.3024 (4)	0.2529 (3)	0.0135 (8)	0.0036 (3)	0.0021 (2)	-0.0012 (8)	0.0014 (6)	-0.0018 (3)
B	-0.501 (1)	0.3632 (8)	0.1942 (6)	0.022 (1)	0.0076 (5)	0.0060 (4)	0.011 (1)	-0.012 (1)	-0.0074 (7)

^a The form of the anisotropic thermal parameter is $\exp[-(B_{11}h^2 + B_{22}k^2 + B_{33}l^2 + B_{12}hk + B_{13}hl + B_{23}kl)]$.

carried out,¹⁰ the present structure will provide important data relevant to the stereochemistry of Rh-diphosphine complexes. In most dpmm complexes the dpmm ligand bridges two Rh atoms,²²⁻²⁶ and, therefore, the four-membered chelate ring with

rhodium is rare. The only other crystallographically characterized M(L-L)₂CO⁺ complex is Ir(dppe)₂CO⁺.¹⁹

X-ray Structure. The crystal structure of [Rh-(dpmm)₂CO]BF₄ consists of discrete, well-separated cations and anions. The shortest cation-cation contact is 3.35 Å for

(22) Olmstead, M. M.; Lindsay, C. H.; Benner, L. S.; Balch, A. L. *J. Organomet. Chem.* **1979**, *179*, 289 and references therein.

(23) Cowie, M. *Inorg. Chem.* **1979**, *18*, 286.

(24) Cowie, M.; Mague, J. T.; Sanger, A. R. *J. Am. Chem. Soc.* **1978**, *100*, 3628 and references therein.

(25) Carré, F. H.; Cotton, F. A.; Frenz, B. A. *Inorg. Chem.* **1976**, *15*, 380.

(26) Nardin, G.; Randaccio, L.; Zangrando, E. *J. Chem. Soc., Dalton Trans.* **1975**, 2566.

Table III. Selected Distances and Angles in $[\text{Rh}(\text{dppm})_2(\text{CO})]\text{BF}_4$

Distances, Å					
Rh-P1	2.322 (2)	P1-C1	1.833 (6)	P2-C1C	1.810 (6)
Rh-P2	2.359 (2)	P2-C1	1.855 (5)	P2-C1D	1.807 (6)
Rh-P3	2.306 (2)	P3-C2	1.840 (6)	P3-C1E	1.820 (6)
Rh-P4	2.383 (1)	P4-C2	1.853 (6)	P3-C1F	1.818 (6)
Rh-C	1.894 (6)	P1-C1A	1.805 (5)	P4-C1G	1.840 (6)
C-O	1.096 (8)	P1-C1B	1.812 (6)	P4-C1H	1.829 (6)
P1-P2	2.691 (2)	P1-P4	3.718 (2)	P3-P2	3.592 (2)
P3-P4	2.713 (2)	P1-C	3.164 (6)	P3-C	3.083 (6)
P2-P4	3.582 (2)	P2-C	4.032 (6)	P4-C	3.697 (6)
B-F1	1.22 (1)	B-F2	1.32 (1)	B-F3	1.19 (2)
B-F4	1.43 (2)				

Angles, Deg					
P1-Rh-P2	70.16 (5)	Rh-P1-C1	94.7 (2)	Rh-P4-C1G	117.9 (2)
P3-Rh-P4	70.67 (5)	Rh-P1-C1A	122.4 (2)	Rh-P4-C1H	128.6 (2)
P4-Rh-C	119.2 (2)	Rh-P1-C1B	116.0 (2)	P1-C1-P2	93.7 (3)
P2-Rh-C	142.7 (2)	Rh-P2-C1	92.9 (2)	P3-C2-P4	94.6 (3)
P2-Rh-P4	98.09 (5)	Rh-P2-C1C	119.1 (2)	C1A-P1-C1B	107.4 (3)
P1-Rh-C	96.8 (2)	Rh-P2-C1D	125.5 (2)	C1C-P2-C1D	104.7 (3)
P1-Rh-P4	104.39 (5)	Rh-P3-C2	95.3 (2)	C1E-P3-C1F	103.5 (3)
P3-Rh-C	93.9 (2)	Rh-P3-C1E	123.1 (2)	C1G-P4-C1H	103.8 (3)
P3-Rh-P2	100.69 (6)	Rh-P3-C1F	115.9 (2)	Rh-C-O	174.7 (7)
P1-Rh-P3	169.27 (6)	Rh-P4-C2	92.4 (2)	F1-B-F4	91 (1)
F1-B-F2	111 (1)	F1-B-F3	129 (2)	F2-B-F3	115 (1)
F2-B-F4	104 (2)	F3-B-F4	98 (2)		

Table IV. Table of Least-Squares Planes^a

plane no.	A	B	C	D	atom	X	Y	Z	dist, Å
1	0.8590	0.3624	-0.3617	0.1211	C ^b	-0.8515	2.3954	0.0429	-0.000
					P2 ^b	-1.9476	6.1107	1.1619	-0.000
					P4 ^b	-0.1137	3.9245	3.3272	0.000
					Rh ^c	-1.0180	3.9425	1.1220	0.027
					P1 ^c	-3.3144	3.8094	1.4388	-2.108
					P3 ^c	1.2312	4.4433	1.0288	2.175
					O ^c	-0.6692	1.5400	-0.6173	0.085
2	-0.1038	0.2596	-0.9601	0.3327	P1 ^b	-3.3144	3.8094	1.4388	-0.381
					P2 ^b	-1.9476	6.1107	1.1619	0.340
					P3 ^b	1.2312	4.4433	1.0288	-0.295
					C ^b	-0.8515	2.3954	0.0429	0.336
					Rh ^c	-1.0180	3.9425	1.1220	-0.281
					P4 ^c	-0.1137	3.9245	3.3272	-2.497

^a Planes were calculated by using unit weights. The equation of the plane is of the form $AX + BY + CZ - D = 0$, where A , B , C , and D are constants and X , Y , and Z are orthogonalized coordinates. ^b Atoms in plane. ^c Other atoms.

C3G...O, and the shortest cation-anion contact is 3.28 Å for C2E...F1. Figure 1 presents a perspective view of the cation, including the numbering scheme. The inner-coordination sphere of the cation is shown in Figure 2 along with some selected distances and angles. Figure 3 presents an ORTEP stereoview of the cation. Distances and angles within the cation are presented in Table III.

In the $\text{Rh}(\text{dppm})_2\text{CO}^+$ cation the coordination geometry about the Rh(I) center is best described as a distorted TBP, with the CO ligand occupying an equatorial site. The two chelating dppm ligands span equatorial and axial positions. Since the "bite" angle (P-Rh-P) of the dppm chelate [average value 70.42 (5)°] is much less than the ideal TBP value of 90°, a significant distortion from the TBP geometry results. However, the Rh atom is displaced only 0.026 Å from the equatorial plane formed by C, P2, and P4 (Table IV, plane 1), the average P1-Rh-equatorial ligand angle is 90.5°, the average P3-Rh-equatorial ligand angle is 88.4°, and the P1-Rh-P3 angle is 169.3°, in reasonable agreement with the requirements of TBP geometry. Attempts to describe the geometry of $\text{Rh}(\text{dppm})_2\text{CO}^+$ as square pyramidal (SP) prove less fruitful. No set of four donor atoms forms a good least-squares plane. The best such basal plane is formed by P1, P2, P3, and C, and distances of these atoms from the least-squares plane are shown in Table IV (plane 2). The best

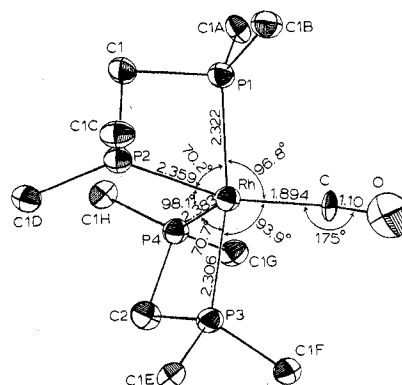


Figure 2. ORTEP perspective (30% probability ellipsoids) of the inner coordination sphere of the cation $\text{Rh}(\text{dppm})_2\text{CO}^+$, including selected distances and angles.

SP description by this criterion and by the requirements of SP geometry that the set of four axial ligand-Rh-basal ligand angles and the set of four basal ligand-Rh-basal ligand angles be equivalent within each set places P4 at the axial site. This choice is qualitatively confirmed by careful examination of the ORTEP stereoview (Figure 3). The lack of planarity in the square base (Table IV) and the large range of values for the

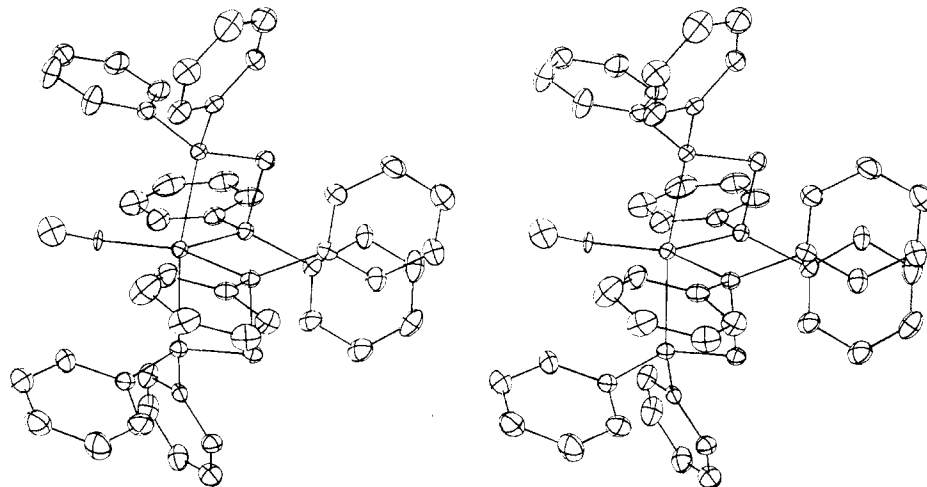


Figure 3. Stereoview of $\text{Rh}(\text{dppm})_2\text{CO}^+$.

P4–Rh–basal angles (70.7 – 119.2° , average 98.1°) and for the basal–Rh–basal angles (70.2 – 100.7° , average 90.4°) makes this geometry description less satisfactory than TBP geometry. However, the actual geometry is clearly intermediate between TBP and SP and is similar to those observed in $\text{Ir}(\text{dppm})_2\text{O}_2^+$ ¹⁸ and $\text{Ir}(\text{dppe})_2\text{CO}^+$.¹⁹

The Rh–P distances (average 2.343 (2) Å) compare favorably with those reported for other rhodium–dppm complexes (2.30 – 2.34 Å).^{10,22–27} However, there are significant differences between the individual Rh–P distances in $\text{Rh}(\text{dppm})_2\text{CO}^+$. The two Rh–P(axial) distances are 2.322 (2) and 2.306 (2) Å and differ by 8σ while the two Rh–P(equatorial) distances are 2.383 (1) and 2.359 (2) Å and differ by 16σ . Although the Rh–P(equatorial) distances are expected to be longer than the Rh–P(axial) distances due to the trans effect of the CO ligand, the differences within the equatorial and axial sets is unexpected. Similar differences between equivalent M–P distances in complexes where dppm chelates to a single metal atom have been noted previously and have been attributed to steric constraints imposed by chelation.²⁸ Another possible cause of this phenomenon is steric interaction between phenyl *o*-H atoms and the C, O, and Rh atoms (vide infra).

Within the equatorial plane the equatorial–Rh–equatorial angles show an unusual variation [C–Rh–P2, 142.7 (2) $^\circ$; C–Rh–P4, 119.2 (2) $^\circ$; P2–Rh–P4, 98.09 (5) $^\circ$] from the ideal TBP value of 120° . This distortion is very similar to that observed in $\text{Ir}(\text{dppe})_2\text{CO}^+$ (143 , 108 , and 109°)¹⁹ and has been attributed to steric interaction between *o*-H atoms and the carbonyl C and Ir atoms. The closest contacts between an *o*-H and Ir and the carbonyl C atom are 3.1 and 2.5 Å, respectively.¹⁹ Phenyl *o*-H positions have been calculated in $\text{Rh}(\text{dppm})_2\text{CO}^+$ by using the well-established C–H distance of 1.10 Å.^{29,30} The closest contacts between an *o*-H atom and Rh are 3.06 and 3.14 Å for H2G and H2C, respectively. H-atom labels are the same as those for the C atoms to which they are attached. The closest contacts between an *o*-H atom and the carbonyl group are as follows: H2B...C, 2.44 Å; H2B...O, 2.49 ; H2G...C, 2.61 ; H2G...O, 2.95 ; H2F...C, 3.01 ; H2F...O, 2.93 . Phenyl rings C and G are nearly coplanar with the TBP equatorial plane (average dihedral angle 12°), and *o*-H atoms from these rings are somewhat close to the Rh atom. However, the more important contacts occur between

o-H atoms and the CO ligand. These contacts are unusually short, and the combined steric effect of these *o*-H atoms is the most probable cause for the observed configuration. The ORTEP stereoview most clearly shows these effects which are dictated by the overall phenyl ring placements. The phenyl rings are positioned so as to minimize interaction between adjacent rings. It is interesting that this same phenomenon takes place in $\text{Ir}(\text{dppe})_2\text{CO}^+$.¹⁹

The dppm four-membered chelate rings are significantly folded about the P–P vector. This puckering is evident from the angles between the P–Rh–P and the P–C–P planes within each chelate ring which are 29.8 and 27.3° for the Rh, P1, P2, C1 and Rh, P3, P4, C2 chelate rings, respectively. In other nonbridged complexes of dppm this puckering varies from 29.8° (angle between MP_2 and CP_2 planes) in $[\text{Ir}(\text{dppm})_2\text{O}_2]\text{PF}_6$ ³¹ to 0° (planar FeP_2C ring) in $\text{Fe}(\text{dppm})(\text{CO})_3$,³² and, therefore, the dppm chelate rings in $\text{Rh}(\text{dppm})_2\text{CO}^+$ are not unusual. There seems to be no obvious correlation between the degree of puckering and other structural parameters within the coordination spheres of the nonbridged dppm complexes thus far examined.^{10,18,28,32,33} In bimetallic complexes where the dppm ligand bridges two metal centers, significant folding within the M–P–C–P–M rings is observed,^{22–27} and it has been suggested that this folding of the methylene groups reflects an attempt to minimize steric interactions.¹⁰ Similar interactions in the nonbridged complexes are probably important, and in $\text{Rh}(\text{dppm})_2\text{CO}^+$ a flattening of the dppm chelate rings would result in even shorter *o*-H–CO contacts.

The P–C distances (both methylene and phenyl) vary between 1.805 (5) and 1.855 (6) Å with an average value of 1.827 Å, well within the range (1.80 – 1.88 Å) observed in nonbridged chelating dppm ligands.^{10,18,28,32,33} The intraligand P–Rh–P angles (average 70.42 (5) $^\circ$) fall within the range previously reported for chelating dppm ligands (67.3 – 73.5°).^{10,18,28,32,33} The Rh–P–C(methylene) and P–C–P angles (average 93.8 (2) and 94.2 (3) $^\circ$, respectively) are significantly distorted from their expected tetrahedral values due to the strain imposed by the four-membered ring and are typical of values previously observed (94.3 – 97.7 and 90.8 – 96.7° , respectively). In contrast, values near 109° are observed when dppm ligands bridge two metals.^{22–27}

The Rh–C distance of 1.894 (6) Å is longer than that usually observed in Rh(I) complexes (typically 1.81 – 1.84 Å),

(27) Kubiak, C. P.; Eisenberg, R. *J. Am. Chem. Soc.* **1977**, *99*, 6129.

(28) Steffen, W. L.; Palenik, G. J. *Inorg. Chem.* **1976**, *15*, 2432.

(29) Otsuka, S.; Yoshida, T.; Matsumoto, M.; Nakatsu, K. *J. Am. Chem. Soc.* **1976**, *98*, 5850.

(30) "Tables of Interatomic Distances and Configuration in Molecules and Ions"; The Chemical Society Press: London, 1958; p 16.

(31) Calculated from the data in ref 18.

(32) Cotton, F. A.; Hardcastle, K. I.; Rusholme, G. A. *J. Coord. Chem.* **1973**, *2*, 217.

(33) Cheung, K. K.; Lai, T. F.; Mok, K. S. *J. Chem. Soc. A* **1971**, 1644.

and the C-O distance of 1.10 (1) Å is short (typically 1.14-1.17 Å).^{22-23,27} The Rh-C-O angle of 174.7 (7)° indicates a slight deviation from linearity. These unusual values may be due to steric interaction between the CO ligand and the phenyl *o*-H atoms (vide supra) or due to some inadequacy in the refinement. Distances and angles within the phenyl rings are normal, and all of the rings are planar within experimental error. The large thermal parameters and the large differences in equivalent distances and angles within the BF₄⁻ anion suggest some disorder. However, an obvious disordered model was not apparent in the final difference Fourier map. The average B-F distance (1.29 (2) Å) and F-B-F angle (108 (2)°) are well within the range of accepted values.

Acknowledgment. Support of this research through a grant from the National Science Foundation is gratefully acknowledged. We also thank the NSF for partial support of our X-ray diffraction and structure-solving equipment (Grant No. NSF CHE7728505). The Matthey Bishop Co. is acknowledged for a generous loan of RhCl₃.

Registry No. [Rh(dppm)₂CO]BF₄, 73574-66-0; [Rh(dppp)₂CO]BF₄, 73610-24-9; [Rh(dppm)₂]BF₄, 53450-78-5; [Rh(dppp)₂]BF₄, 70196-21-3; Rh₂Cl₂(COD)₂, 12092-47-6.

Supplementary Material Available: Table II (root-mean-square amplitudes of thermal vibration) and a listing of observed and calculated structure factor amplitudes (23 pages). Ordering information is given on any current masthead page.

Contribution from the Department of Chemistry,
New Mexico State University, Las Cruces, New Mexico 88003

Kinetics of Reduction of Metal Complexes by Dithionite

R. N. Mehrotra¹ and R. G. Wilkins*

Received November 20, 1979

Dithionite is used extensively for the reduction of proteins, and there have been recently a number of kinetic studies of these reactions.² By contrast, there have been limited investigations of reactions of dithionite with metal complexes.³⁻⁵ One of the very interesting features of dithionite ion is its ability to reduce as the intact S₂O₄²⁻ ion and/or via the dissociated anion radical SO₂⁻.³ We report here on the reduction of 11 cobalt(III) complexes of a variety of types, as well as the Fe(EDTA)⁻ and Mn(CyDTA)⁻ ions.⁶

Experimental Section

Complexes were prepared by literature methods (see Table I).⁷⁻²¹

- (1) On leave from Department of Chemistry, University of Jodhpur, Jodhpur India.
- (2) P. C. Harrington, D. J. A. deWaal, and R. G. Wilkins, *Arch. Biochem. Biophys.*, **191**, 444 (1978), and references therein.
- (3) D. O. Lambeth and G. Palmer, *J. Biol. Chem.*, **248**, 6095 (1973).
- (4) R. F. Pasternack, M. A. Cobb, and N. Sutin, *Inorg. Chem.*, **14**, 866 (1975).
- (5) J. C. Cassatt, M. Kukuruzirska, and J. W. Bender, *Inorg. Chem.*, **16**, 3371 (1977).
- (6) Abbreviations: IDA = iminodiacetate; EDTA = ethylenediamine-*N,N,N',N'*-tetraacetate; CyDTA = *trans*-1,2-cyclohexanediamine-*N,N,N',N'*-tetraacetate; MEDTA = *N*-methylethylenediamine-*N,N,N',N'*-triacetate; NTA = nitrilotriacetate, terpy = 2,2',2''-terpyridine.
- (7) J. Hidaka, Y. Shimura, and R. Tsuchida, *Bull. Chem. Soc. Jpn.*, **35**, 567 (1962).
- (8) R. A. Rader and D. R. McMillin, *Inorg. Chem.*, **18**, 545 (1979).
- (9) F. P. Dwyer, E. C. Gyrfas, and D. P. Mellor, *J. Phys. Chem.*, **59**, 296 (1955).
- (10) F. P. Dwyer and F. L. Garvan, *J. Am. Chem. Soc.*, **83**, 2610 (1961).
- (11) F. P. Dwyer and F. L. Garvan, *J. Am. Chem. Soc.*, **80**, 4480 (1958).
- (12) C. W. Van Saun and B. E. Douglas, *Inorg. Chem.*, **7**, 1393 (1968).
- (13) M. H. Evans, B. Grossman, and R. G. Wilkins, *Inorg. Chim. Acta*, **14**, 59 (1975).

Table I. Activation Parameters for Reduction by S₂O₄²⁻ (*k*₂) and SO₂⁻ (*k*₃) Ions at 25 °C, pH 7.0, and *I* = 0.4 M

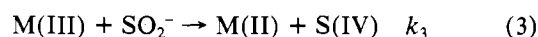
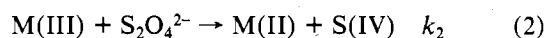
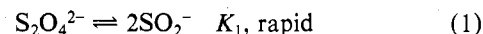
complex ion ^a	<i>k</i> ₂ , ^b M ⁻¹ s ⁻¹	<i>k</i> ₃ , ^b M ⁻¹ s ⁻¹	Δ <i>H</i> [‡] , ^c kcal mol ⁻¹	Δ <i>S</i> [‡] , ^c eu
<i>cis</i> -Co(IDA) ₂ ^{-7,8}	1.9	≤10 ³	15.4	-6
<i>trans</i> -Co(IDA) ₂ ^{-7,8}	1.6	≤10 ³	14.0	-11
Co(EDTA) ⁻⁹	≤0.1	1.0 × 10 ³	17.4	-7
	≤0.1	1.3 × 10 ³ ^d		
Co(CyDTA) ⁻¹⁰	≤0.1	2.3 × 10 ³		
Co(EDTA)Cl ²⁻¹¹	<10	2.1 × 10 ⁵	15.5	-3
Co(MEDTA)Br ^{-12,13}	≤10 ²	6.5 × 10 ⁶ ^e	13.0 ^e	-4 ^e
	≤0.1	1.3 × 10 ⁴ ^f	10.5 ^f	-24 ^f
Co(MEDTA)OH ₂ ^{12,13}	≤0.4	1.5 × 10 ⁴		
Co(C ₂ O ₄) ₃ ³⁻¹⁴	≤0.4	1.8 × 10 ⁴	14.9	-9
		1.0 × 10 ⁴ ^d		
[Co(C ₂ O ₄) ₂ OH] ₂ ^{4-15,16}	≤0.1	1.6 × 10 ⁴	18.4	+2
[Co(NTA)OH] ₂ ^{2-17,18}	≤0.1	4.6 × 10 ³		
Co(terpy) ₂ ³⁺¹⁴	4.3 × 10 ⁵	≤10 ⁷	17.0	+24
Fe(EDTA) ⁻²⁰	3.6 × 10 ⁴	≤2 × 10 ⁶	13.7	+8
Mn(CyDTA) ⁻²¹	2.1 × 10 ⁶	≤10 ⁸		

^a Abbreviations are listed in ref 6, and references to preparation are superscripted. ^b Calculated from experimental value of *K*₁^{1/2}*k*₃ with *K*₁ = 1.4 × 10⁻⁹ M.³ ^c Activation parameters from either log *k*₂ or log (*K*₁^{1/2}*k*₃) vs. 1/*T* plot. Δ*H*[‡] = ±1 kcal mol⁻¹ and Δ*S*[‡] = ±3 eu are the approximate errors for most systems. ^d pH ~10.0. ^e Fast reacting component. ^f Slow reacting component.

The kinetics were studied by using a Beckman 24 spectrophotometer or a Gibson-Durrum stopped-flow apparatus, and serum cap sealed cells and anaerobic conditions were maintained throughout the experiments. The reactions of the cobalt(III) complexes (100 μM-2.0 mM) with dithionite (1-30 mM) were examined in the 530-600-nm region. For the rapid reactions of the Co(terpy)₂³⁺, Fe(EDTA)⁻, and Mn(CyDTA)⁻ ions, 10-100 μM complex and 50 μM-4 mM dithionite were employed with observations at 450, 400, and 510 nm, respectively. Two rates, easily separable, were obtained with the isomeric mixture¹³ in Co(MEDTA)Br⁻. Changes in wavelength or concentrations of complex were without effect on the pseudo-first-order rate constants measured. The majority of the studies were at 25.0 °C, pH 7.0 (maintained with TRIS) and *I* = 0.4 M. Full kinetic data are contained in Table II.²²

Results

Spectral examination of the products of reduction by dithionite indicated formation of the corresponding bivalent metal ion complex(es). The kinetic scheme in eq 1-3 can be



applied to dithionite reduction of the complexes (designated M(III)) for which the rate law (4) applies. With all com-

$$\text{rate}/[\text{M(III)}] = k_{\text{obsd}} = k_2[\text{S}_2\text{O}_4^{2-}] + k_3K_1^{1/2}[\text{S}_2\text{O}_4^{2-}]^{1/2} \quad (4)$$

plexes examined,²³ plots of either *k*_{obsd} vs. [S₂O₄²⁻] or *k*_{obsd} vs.

- (14) J. C. Bailar, Jr., and E. M. Jones, *Inorg. Synth.*, **1**, 37 (1939).
- (15) A. W. Adamson, H. Ogata, J. Grossman, and R. Newbury, *J. Inorg. Nucl. Chem.*, **6**, 319 (1958).
- (16) L. Hin Fat and W. C. E. Higginson, *J. Chem. Soc. A*, 298 (1967).
- (17) M. Mori, M. Shibata, E. Kyuno, and Y. Okubo, *Bull. Chem. Soc. Jpn.*, **31**, 940 (1958).
- (18) D. R. Meloon and G. M. Harris, *Inorg. Chem.*, **16**, 434 (1977).
- (19) B. R. Baker, F. Basolo, and H. M. Neumann, *J. Phys. Chem.*, **63**, 371 (1959).
- (20) H. J. Schugar, A. T. Hubbard, F. C. Anson, and H. B. Gray, *J. Am. Chem. Soc.*, **91**, 71 (1969).
- (21) R. E. Hamm and M. A. Suwyn, *Inorg. Chem.*, **6**, 139 (1967).
- (22) Supplementary material.